Received: December 8, 2021. Revised: March 15, 2022.

International Journal of
Intelligent Engineering & Systems

http://www.inass.org/

Robust Reversible Watermarking using Stationary Wavelet Transform and Multibit Spread Spectrum in Medical Images

Ledya Novamizanti[1,2]* **Andriyan Bayu Suksmono[1]**
Donny Danudirdjo[1] **Gelar Budiman[2]**

[1] Doctoral Program of Electrical Engineering and Informatics,
School of Electrical Engineering and Informatics, Institut Teknologi Bandung, Indonesia
[2]School of Electrical Engineering, Telkom University, Bandung, Indonesia
* Corresponding author's Email: ledyaldn@telkomuniversity.ac.id

Abstract: In medical applications, the slightest distortion in the patient's medical image cannot be tolerated, as such distortion can lead to misdiagnoses and misleading conclusions. The robust reversible watermarking technique has received considerable attention, as it allows the complete extraction of the embedded watermark signal and the comprehensive reconstruction of the masking signal. This paper proposes a robust reversible watermarking (RRW) scheme based on Stationary Wavelet Transform (SWT) and Multibit Spread Spectrum (MSS). The host image is broken down into several subbands using SWT. Then, the watermark is embedded into the subband diagonal detail coefficient of the host image using MSS. Finally, the watermarked subband is combined with other subbands using inverse SWT (ISWT) into a watermarked image. The embedded watermark is extracted on the receiving side, and the original medical image is precisely reconstructed without involving auxilary information. By the experimental results, the proposed robust reversible watermarking technique can restore the watermark and rebuild the host medical image perfectly without any attack. The watermarked images produced by the proposed reversible data hiding technique have better visual quality with a peak signal-to-noise ratio above 41 dB. In addition, the proposed RRW scheme is robust to various attacks such as compression, noise addition, sharpening, and image enhancement.

Keywords: Robust, Reversible, Singular wavelet transform, Spread spectrum, Watermarking.

1. Introduction

The high-speed development of information and communication technology has resulted in quickly sending digital data from one area to another. Transmission of medical data over public networks causes security issues such as modification, deletion, unauthorized access, forgery by unauthorized persons. Medical information is susceptible and valuable because it is needed for diagnosis, treatment, and research [1]. Digital image watermarking is one solution to preserve medical images and their ownerships from providing high security and privacy [2, 3].

The electronic patient record (EPR) is integrated into the medical image during watermarking, with no visible modifications to the medical image. The slightest distortion of the patient's medical image is not tolerated because such distortion can lead to misdiagnoses and misleading conclusions that are even very dangerous for a person's life [4]. The reversible watermarking technique has received considerable attention, as it allows the complete extraction of the watermark signal and the perfect reconstruction of the host signal. In contrast, the host signal is lost in conventional watermarking, and only the watermark signal can be recovered [5].

Reversible watermarking schemes are fragile, which means they don't handle any attack at all. This scheme works in a scenario that assumes a noise-free communication channel in transmitting a watermarked signal. However, in reality, attacks are an unavoidable condition in communication channels [5]. Therefore, lossless information hiding, called the powerful reversible watermarking scheme, is necessary for the safe transmission of medical images [6].

Thabit et al. presented a Slantlet transformation (SLT)-based RRW system in [7]. The image is separated into blocks that do not overlap. Then, using SLT, each block is converted. To transmit watermark information, the mean values of specified high-frequency subbands are modified. This technique is resistant to compression, additive Gaussian noise (AGN), and salt and pepper noise, as well as histogram sharpening and equalization to some extent. However, the watermarked image's quality is poor, with an average PSNR of 29 dB for a capacity of 1024 bits in medical photographs. Selvam *et al.* [6] describe a blind hybrid reversible watermarking method that works in the transform domain to boost concealing capacity and preserve medical images. Watermarks in medical photographs are encoded using the IWT, and the Discrete Gould transform (DGT). On extraction, the concealed watermark is revealed, and the original, unaltered image is recovered without the need for any further data. However, this method has a significant degree of distortion and a poor payload capacity.

This paper proposes robust and reversible watermarking (RRW) on medical images based on Stationary Wavelet Transform (SWT). The SWT upsampling property can store more context information so that it can apply to reversible watermarking. The SWT method does not require a downsampling procedure but instead adopts a zero placement procedure [8, 9]. The strong point of this proposed scheme is the reversible watermarking scheme with a balanced trade-off between imperceptibility and robustness by embedding the watermark into the high-frequency sub-band of SWT. The pseudo-noise (PN) code is generated along the watermark bits. Then, the watermark bit is mapped that corresponds to the PN code index and embedded using a Multibit Spread Spectrum (MSS). Finally, the watermarked subband is combined with other subbands using inverse SWT (ISWT) into a watermarked image. At the receiving end, the watermarked image is divided into non-overlapping blocks, and SWT is performed. The watermark is detected by finding the maximum correlation of the corresponding PN code. Then, the host image is obtained by reconstructing it with ISWT.

The paper will be organized as follows in the next part. The associated investigations are briefly discussed in Section 2. The ideas of SWT and MSS are discussed in Section 3. The suggested robust reversible watermarking technique's embedding and extraction strategies are described in Section 4. Section 5 contains the experimental data and comments. Finally, in Section 6, we present our conclusions.

2. Related works

This section briefly describes related studies that discuss robust and reversible watermarking techniques on images. Robust watermarking methods are used for proprietary or copyright protection purposes, so they must be resistant to various attacks. Setyono and Setiadi [10] proposed an image watermarking technique based on Discrete Tchebichef Transform (DTT) and Singular Value Decomposition (SVD). The advantages of these two transformations are that DTT has a faster computation time than the Discrete Cosine Transform (DCT), and SVD is resistant to signal processing and geometry attacks. In the initial stage, the Arnold transformation is applied to the host image to increase the security of the watermark. Then, divide the host image into 8×8 non-overlapping blocks. Each block is used DTT, and only the lowest coefficient is taken. The watermark is embedded in the SVD singular matrix in the next step. The proposed technique was tested on six standard images, resulting in high visual quality with a mean PSNR of 45 dB and SSIM 0.9. The fundamental weakness of this proposed technique is that the watermarking method is non-blind. The host image is required at the time of watermark extraction.

Novamizanti *et al*. [11] reported a watermarking scheme on medical images that combines three transformations: Fast Discrete Curvelet Transforms (FDCuT), DCT, and SVD. First, the medical host image was processed using FDCuT. In the high-frequency subband of FDCuT, medical host images were divided into 8x8 non-overlapping blocks, and DCT was applied. Simulations are carried out using twelve medical images from four modalities, namely Magnetic resonance imaging (MRI), Computed tomography (CT), X-ray, and ultrasound (US). The experimental results show higher visual quality in the watermarked image with a mean PSNR of 54 dB. and SSIM 0.9. Watermarking schemes based on FDCuT, DCT, and SVD produce watermarks resistant to compression and signal processing attacks. A similar weakness is experienced by this study, where the proposed watermarking technique is semi-blind, which means that a watermark is required during the extraction process.

Mohammed *et al.* [12] improve the performance of [11] and [13] by eliminating the DCT process and using the gain factor coefficient for the watermark insertion and extraction steps. Radon Transform (RT) is applied to the watermark for added security. The experimental results showed the imperceptibility of watermarked medical images with a mean PSNR of 57 dB for all medical images obtained from the Medpix database. This proposed scheme has shown better resistance than [11] and [13] but is still limited to geometrical attacks. In addition, this scheme is semi-blind when extracting the singular value of the watermark image is required.

The robust watermarking technique [10-13] only recovers the watermark signal while the host signal is lost. Meanwhile, the RRW scheme can extract the watermark and host signals without attack. Thabit and Khoo [14] presented a reversible authentication technique on medical images. The proposed approach uses SLT to embed watermark information in the Region of Interest (ROI) and Region of Non-Interest (RONI). Robust watermarks are embedded in ROI, and reversible watermarks for tamper detection, localization, and recovery are embedded in RONI. The ROI region was divided into non-overlapping 16×16 blocks, and each block's average intensity was calculated. After that, the Integer Wavelet Transform (IWT) coefficient was applied to obtain ROI recovery information. The information extracted from the ROI is then embedded in the RONI. The main limitation of this technique is that the tampered area cannot be detected without the average block intensity, and there is a need for additional information along with the watermark image on the decoder side, thereby increasing unnecessary overhead for the technique.

Liu *et al*. [15] presented ROI and RONI-based reversible watermarking techniques to protect medical imaging content from modification. Recursive Dither Modulation (RDM) is combined with SLT and SVD transformations to protect image authenticity. ROI region is used for watermarks with a practical recovery function under limited embedding capacity. Then, the watermark is embedded throughout the medical image. The experimental results represent that the proposed scheme has a high imperceptibility and a mean PSNR of 41 dB. This scheme has the drawback of false-positive errors during the watermark extraction stage. The reason is the use of significant values in the SVD singular matrix in the watermark embedding technique. The quantization step should be set to a sufficient value to achieve a spectacular trade-off between watermarking resilience and imperceptibility. When the quantization step is more extensive, the watermark robustness increases, but the watermark imperceptibility decreases.

Wang *et al*. [16] proposed an independent embedding domain (IED)-based two-stage RRW scheme. First, the cover image is changed to two IEDs, i.e., low and high frequency. The robust watermark is pinned to the low frequency, and the reversible watermark is pinned to the high frequency. The verification results from the experiment showed high imperceptibility with a mean PSNR of 43 dB in the three standard images. High resistance to robust watermarks against compression attacks, AWGN, and Gaussian filters, but not resistant to median and wiener filter attacks.

Furthermore, we introduce a related study that uses SWT and SS for image watermarking. SWT has been applied to image watermarking [17, 18], but the proposed scheme is not reversible. Nagarjuna and Ranjeet [17] combined the information from the low-frequency SWT coefficient and the watermark image without modifying the information contained in the original image. To extract the watermark, we need a key derived from the results of the SWT low-frequency coefficient and the watermark. The simulation results of the proposed scheme have shown good perception and resilience across various watermarking attacks. Dai *et al*. [18] offered SWT-DCT to extract visual feature vectors from medical images for embedding and extracting watermarks. The zero watermark concept is applied so that the watermark can withstand conventional attacks and geometric attacks.

In the discrete wavelet transform (DWT) domain, Kumar *et al*. [19] used a SS to introduce a text watermark onto a digital radiological image. Before embedding, the BCH error correction code is applied to the ASCII formatted text watermark to increase its durability. The suggested method enables invisible watermarking for string watermarks, and the use of BCH codes can reduce bit errors in the recovered watermarks, according to simulation findings. The proposed scheme is robust against various attacks such as compression, filtering, noisy image, sharpening, and histogram equalization. However, the system only manages to recover the watermark during extraction. Maity and Kundu [20] proposed SS image watermarking schemes using several wavelets transform combined with various modulation, multiplexing, and signaling techniques. In the case of two-band systems, data embedding in the LL and HH subbands offers better spectrum spread and higher robustness. Samcovic and Milovanovic [21] also applied a discrete wavelet transform to the original host image. Then, a spread spectrum technique is used to embed the watermark into the original image. The experimental results show that DWT and SS in embedding watermarks can provide high performance. The watermark does not distort the image quality by considering the value of the obtained PSNR as an objective assessment for

Received: December 8, 2021. Revised: March 15, 2022.

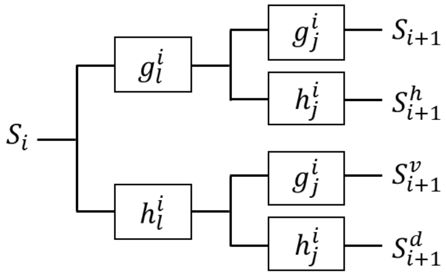

Figure. 1 Illustration of SWT filter bank two levels decomposition

an image. However, the proposed scheme has not tested the robustness of the watermark against various forms of attack and only succeeded in recovering the watermark during extraction.

3. Preliminary

In this section, we briefly introduce stationary wavelet transform (SWT) and multibit spread spectrum (MSS), both of which are used in our proposed scheme.

3.1 Stationary wavelet transform

Based on multi-scale and multi-direction, SWT suggested by Nason and Silverman demonstrates redundancy and shift-invariance features. SWT does not obliterate the original signals and alters at each level by padding them out with zeros, rather than implementing the down-sampling process after applying the low-pass (LP) and high-pass (HP) filters to the signal such as the image. Accordingly, the new image is the same resolution as the approximation signal at higher levels, and shift-invariance is obtained at the expense of redundant decomposition. SWT also has a low computational cost despite its redundancy [8]. SWT is used for this investigation for the reasons stated above. Fig. 1 depicts the SWT decomposition process.

Consider $f(x,y)$ an image with size H × W. The mathematical equation of decomposition at the level i of SWT is as follows [8]:

$$\begin{cases} S_{i+1}(a,b) = \sum_j \sum_l g_j^i\, g_l^i\, S_i(a+j, b+l) \\ S_{i+1}^h(a,b) = \sum_j \sum_l h_j^i\, g_l^i\, S_i(a+j, b+l) \\ S_{i+1}^v(a,b) = \sum_j \sum_l g_j^i\, h_l^i\, S_i(a+j, b+l) \\ S_{i+1}^d(a,b) = \sum_j \sum_l h_j^i\, h_l^i\, S_i(a+j, b+l) \end{cases} \quad (1)$$

with $a = 1,2,\dots,H$ and $b = 1,2,\dots,W$, g_j^i and g_l^i are LP filters, h_j^i and h_l^i are HP filters, S_i and S_{i+1} represent the low frequency subband at level i and $i+1$, respectively. While, S_{i+1}^h, S_{i+1}^v, and S_{i+1}^d are the horizontal, vertical and diagonal detail coefficients at level $i+1$, respectively.

The formula of invers SWT can be calculated as follows [8]:

$$\begin{aligned} \tilde{S}_i(a,b) = &\sum_j \sum_l \tilde{g}_j^i\, \tilde{g}_l^i\, \tilde{S}_{i+1}(a+j, b+l) \\ &+ \sum_j \sum_l \tilde{h}_j^i\, \tilde{g}_l^i\, \tilde{S}_{i+1}^h(a+j, b+l) \\ &+ \sum_j \sum_l \tilde{g}_j^i\, h_l^i\, \tilde{S}_{i+1}^v(a+j, b+l) \\ &+ \sum_j \sum_l \tilde{h}_j^i\, \tilde{h}_l^i\, \tilde{S}_{i+1}^d(a+j, b+l) \end{aligned} \quad (2)$$

where $\tilde{g}_j^i$ and $\tilde{g}_l^i$ are the reconstruction of LP filters, $\tilde{h}_j^i$ and $\tilde{h}_l^i$ are the reconstruction of HP filters, $\tilde{S}_i$ and $\tilde{S}_{i+1}$ are the reconstruction low frequency subband at level i and $i+1$, respectively. While, $\tilde{S}_{i+1}^h$, $\tilde{S}_{i+1}^v$, and $\tilde{S}_{i+1}^d$ are the reconstructed of horizontal, vertical and diagonal detail coefficients, respectively.

3.2 Multibit spread spectrum

The amount of hidden data can be increased by inserting a multibit spread spectrum (MSS)-based watermark. Given a host signal $\boldsymbol{X} = (\bar{X}_1, \bar{X}_2, \dots, \bar{X}_L)$ and watermark $\boldsymbol{W} = (\bar{W}_1, \bar{W}_2, \dots, \bar{W}_L)$. The motivation of this technique is to design the embedding function E so that N messages are hidden in host signal $\boldsymbol{X}$. Thus, a watermarked signal $\overline{\overline{\boldsymbol{X}}} = \left(\overline{\overline{X_1}}, \overline{\overline{X_2}}, \dots, \overline{\overline{X_L}}\right)$ is obtained. On the receiving end, messages can be extracted from $\overline{\overline{\boldsymbol{X}}}$ without involving $\boldsymbol{X}$.

The multibit spread spectrum technique based on PN code [22] works by independently generating a random code with a Gaussian $\mathcal{N}(0,1)$ of 2^N. The N bits of data to be embedded to $\boldsymbol{X}$ modulate the PN code W_p. Mathematically, message m can be added additively to host signal $\boldsymbol{X}$ using the following equation [23]:

$$\overline{\overline{\boldsymbol{X}}} = E(\boldsymbol{X}, m) = \boldsymbol{X} + \boldsymbol{\alpha}\, \boldsymbol{W}_m \quad (3)$$

with $\overline{\overline{\boldsymbol{X}}}$ represents the watermarked signal and $\boldsymbol{\alpha}$ is a gain factor to control the tradeoff between imperceptibility and watermark robustness as a requirement of watermarking applications.

On the receiving end, the challenge is extracting the embedded information in $\overline{\overline{\boldsymbol{X}}}$. If the host signal $\boldsymbol{X}$ successfully generates a Gaussian distributed PN code, then the linear correlator function is applied in the extraction process. Suppose $\boldsymbol{W}_0, \dots, \boldsymbol{W}_{M-1}$ is a PN code that is generated again the same as during the insertion process, and $Corr\left(\overline{\overline{\mathbf{X}}}, \mathbf{W}_\mathrm{i}\right)$ is a linear correlation between the reference code and the watermarked signal [24]. The embedded information is encoded in the index of the reference code, which is the maximum correlation with the watermarked signal. The reconstruction of m is formulated as follows [23]:

$$\widetilde{m} = \underset{i\epsilon\{0,\dots,M-1\}}{arg\ max}\ Corr\left(\widetilde{\widetilde{\boldsymbol{X}}}, \boldsymbol{W}_i\right) \quad (4)$$

4. Proposed scheme

This paper proposes an RRW scheme for medical images that offers high resistance and imperceptibility with high capacity. Fig. 2 shows the proposed reversible watermarking scheme on general medical pictures. In the embedding process, the medical image of the original host $\boldsymbol{X}$ is decomposed into various subbands via SWT. The selected subband from SWT is used as the insertion area using Multibit Spread Spectrum (MSS) [25]. After the watermark is restored $\widetilde{\boldsymbol{W}}$, the host image $\boldsymbol{X}$ can be reconstructed from the watermarked image $\boldsymbol{Y}$. In the ideal case, when no attack occurs during transmission, the recovered watermark $\widetilde{\boldsymbol{W}}$ equals the inserted watermark $\boldsymbol{W}$.

4.1 Embedding stage

This section reports the embedding of a watermark in an agency logo or EPR image into the host medical image. The watermark is embedded into the selected subband of SWT on the host medical image. Then a PN code-based watermark is inserted into the transformed host using the MSS technique. The output of the embedding process is a watermarked medical image. Fig. 3 illustrates the embedding technique from this paper.

The stages of the watermark embedding technique into medical images are as follows:

1. Read the medical host image $\boldsymbol{X}$ of size $H \times W$ and the image of the watermark $\boldsymbol{W}$. This medical original image is divided into non-overlapping $B \times B$ sized blocks. While the watermark size L_w is $n_b \times H \times W/B^2$ with the number of watermark bits contained in each block is denoted by n_b.
2. Apply SWT to $\boldsymbol{X}$ using Eq. (1), which decomposes the host image into four frequency subbands: $\boldsymbol{X}_a, \boldsymbol{X}_h, \boldsymbol{X}_v$, and $\boldsymbol{X}_d$. The selected subband, the diagonal detail coefficient $\boldsymbol{X}_d$, is used as the watermark insertion area. Subband analysis is described in the next section.
3. Generate PN code with Gaussian distribution of size $2^{nb} \times B^2$. For each block of $\boldsymbol{X}_d$, the watermark bit is mapped into the pn code, so $\boldsymbol{W}_p$ is obtained.
4. Embed the watermark $\boldsymbol{W}_p$ into $\boldsymbol{X}_d$ using MSS, with the following formulation:

$$\boldsymbol{Y} = \boldsymbol{X}_d + \alpha\, \boldsymbol{W}_p \quad (5)$$

with $\boldsymbol{Y}$ is the watermarked image and α is the gain factor. Then, apply the SWT inverse of $\boldsymbol{Y}$ using Eq. (2), to obtain a watermarked medical image $\widehat{\boldsymbol{Y}}$.

4.2 Extraction stage

This section describes the essential tasks of the extraction process for reversible watermarking, namely, retrieval of watermark images and host images when the transmission channel is not attacked. In general, the extraction technique performs the reverse process of the insertion technique. In the ideal case, when there is no attack on the transmission channel, the recovered watermark $\boldsymbol{W'}$ is the same as the inserted watermark $\boldsymbol{W}$. Fig. 4 illustrates the extraction technique of this study.

The stages of the watermark extraction technique are as follows:

1. Read the watermarked medical image $\boldsymbol{Y}$. It is divided into non-overlapping $B \times B$ sized blocks.
2. Apply SWT to $\boldsymbol{Y}$ using Eq. (1), which watermarked medical image into four frequency subbands: $\boldsymbol{Y}_a, \boldsymbol{Y}_h, \boldsymbol{Y}_v$, and $\boldsymbol{Y}_d$. The diagonal detail coefficient $\mathbf{Y}_\mathrm{d}$ is the watermark embedding location.
3. Calculate the maximum correlation of the multiplication of PN code and $\boldsymbol{Y}_d$ using Eq. (4). The watermark $\boldsymbol{W}$ is detected from the index with the maximum correlation.
4. The medical image is recovered by the inverse function of Eq. (4), as follows:

$$\boldsymbol{X}_d = \boldsymbol{Y}_d - \alpha\, \boldsymbol{W} \quad (6)$$

where $\boldsymbol{X}_d$ is the recovered medical image, that is,

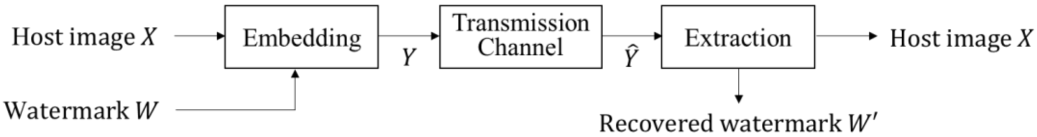

Figure. 2 The proposed reversible watermarking scheme in general

Received: December 8, 2021. Revised: March 15, 2022.

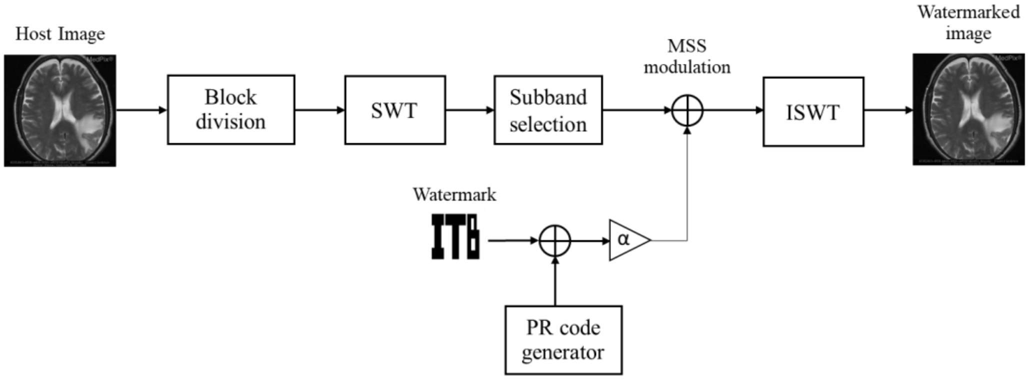

Figure. 3 The embedding process on SWT and MSS-based RRW

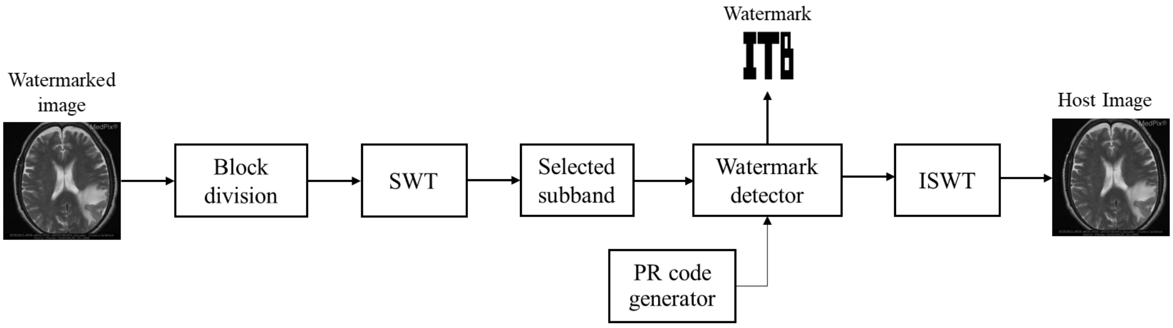

Figure. 4 The extraction process on SWT and MSS-based RRW

in the coefficient of detail, and α is the gain factor. Then apply the SWT inverse of $\boldsymbol{X}_d$ using Eq. (2) to obtain the recovered medical image.

5. Result and discussion

This section discusses the conduct of the proposed RRW technique. The test of this technique uses an image of a medical host in grayscale format and has a size of 512×512 pixels. A total of four medical images were carried out as test data, including MRI, X-Ray, Computed Tomography (CT), and Ultrasound (US). The medical images are taken from the MedPix™ Medical Image Database [26]. The type of host image modality used is shown in Fig. 5 (a-d). Meanwhile, the ITB logo image was chosen as a watermark whose size depends on the parameters n_b and B, as discussed in the previous section. Based on the experimental results, we set as many as four bits to be embedded in each 32×32 non-overlapping block based on the combination of the number of bits and the block size. Thus, the size of the watermark that is inserted into the original host medical image is $4 \times 512^2/32^2 = 1024$ bits. The efficiency of the proposed scheme is thoroughly evaluated on three watermarking criteria: imperceptibility, reversibility, and robustness.

The Peak Signal to Noise Ratio (PSNR) is a measurement for determining visual imperceptibility. PSNR is primarily concerned with the visual resemblance of the original and watermarked images. The two images should look the same so that there is no significant difference between the two. The higher the PSNR value, the more similar the two images are, and vice versa. Consider that $\boldsymbol{X}$ is the original host image, $\boldsymbol{Y}$ is the watermarked host image, and $H \times W$ is the size of the host image. Mathematically, PSNR (in dB) is formulated as follows [13]:

$$PSNR = 10\ log \frac{255^2 \times H \times W}{\sum_{i=1}^{H} \sum_{i-1}^{W} (\boldsymbol{X} - \boldsymbol{Y})^2} \quad (7)$$

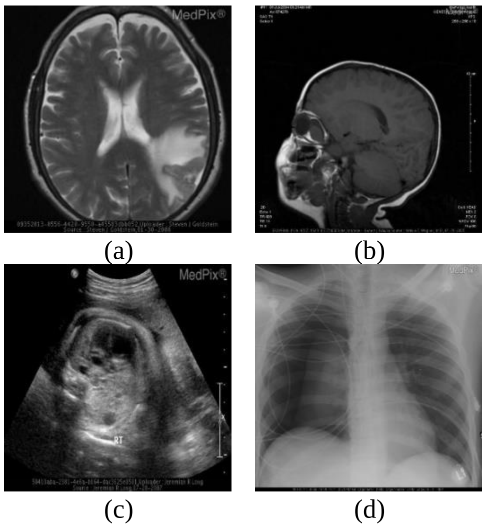

Figure. 5 Four modalities of original medical image: (a) CT, (b) MRI, (c) US, and (d) X-Ray.

Received: December 8, 2021. Revised: March 15, 2022.

Bit Error Rate (BER) and Normalized Cross Correlation (NC) are benchmarks used to evaluate the robustness of a proposed medical image watermarking scheme against attacks. Technically, BER measures the bit error rate after the watermark extraction process. If the value of BER is close to 0, then the bit error rate is low, and vice versa. Ideally, the BER value should be 0. Given that IB is the number of wrongly decoded bits and TB is the total number of watermark bits, BER can be expressed mathematically as follows [16]:

$$BER = \frac{IB}{TB} \tag{8}$$

Mathematically, NC can be calculated as follows:

$$NC = \frac{\sum_{i=1}^{H}\sum_{j=1}^{W}(w \times w')}{\sum_{i=1}^{H}\sum_{j=1}^{W} w^2} \tag{9}$$

If the NC value is away from 0, then the resistance of the watermarking system is fragile. On the other hand, if NC is 1, the watermarking scheme is said to be robust. The increase of the NC value, then the higher correlation between the original watermark w and the recovered watermark w'. The NC value must be above 0.9 for the scheme to withstand attacks [2].

5.1 Parameter evaluation

5.1.1. SWT Subband

In this section, the SWT subband test is carried out on the RRW performance. Approximation, Horizontal, Vertical, and Detail are the four subbands of SWT output. Fig. 5 shows an illustration of SWT on a CT image. And also, Table 1 tabulates the watermarking performance metrics for the SWT subband evaluation.

The SWT subband type test results in Table 1 show that the PSNR metric value achieved is significant because of PSNR>40 dB for all SWT subbands. The perceptual impermanence for the proposed approach is characterized by calculating a PSNR that is well above 35 dB. BER and NC metrics reach ideal values in the detail subband coefficient, namely BER is 0 and SSIM is 1. The bit error ratio after the watermark extraction process is calculated

Table 1. Comparison of subband performance

Subband	PSNR (dB)	BER	NC
Approximation	41.5144	0.4141	0.6442
Horizontal	41.6733	0.0498	0.9283
Vertical	41.6711	0.0400	0.9596
Detail	41.5081	0	1

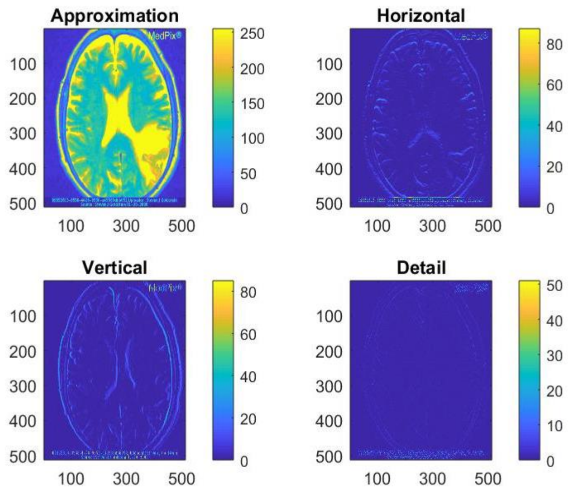

Figure. 6 Ilustration of SWT on CT image

using BER. The BER value is 0, which means the watermark is successfully restored on the receiving end. In Fig. 6, all of the detail subband coefficients have an intensity of 0. In this subband, the watermark is completely restored. In the detail subband coefficient, the average PSNR value is 41.5081 dB, around 41 dB. Therefore, the detail subband was chosen because it produces the best watermarking performance among other subbands.

5.1.2. Gain factor α

This section examines the gain factor on the performance of watermarking. The value of tested ranges from 0 to 12. Fig. 7 shows the watermarking performance metric for testing the gain factor. Fig. 7(a) visually displays the effect of on BER. Fig. 7(b) shows the impact of α on BER and PSNR.

The gain factor α determines the strength of the watermark embedding into the host medical image. In the insertion process, the parameter α is applied in Eq. (4). Experiments were carried out on four medical image modalities. Based on Fig. 7(a), the higher the α value, the lower the BER obtained. At α >6, BER equal to zero is obtained. It means that the restored watermark is acceptable on the receiving end. The resulting BER value 0 means that there are no bit errors in the watermark during the extraction process. In Fig. 7(b), under ideal conditions, namely BER is zero, and the range of PSNR values is above 35 dB to 43 dB. The higher the PSNR, the lower the watermark resistance. The results of the watermarked image and the PSNR performance for the four medical image modalities are shown in Fig. 7. The average PSNR generated for the four medical image modalities is 42.4097 dB. It is indicated that the proposed RRW performance provides an acceptable imperceptibility.

5.2 Reversibility evaluation

In this subsection, we examine the reversibility of the proposed RRW scheme. The reversibility is evaluated from the difference between the original and the recovered medical images [27]. Fig. 8 represents an illustrative example of a test data with the performance of the extracted host medical images. The experimental and visualization results show no difference between the original and the recovered medical images. All hosted medical images and watermarks can be salvaged without data loss.

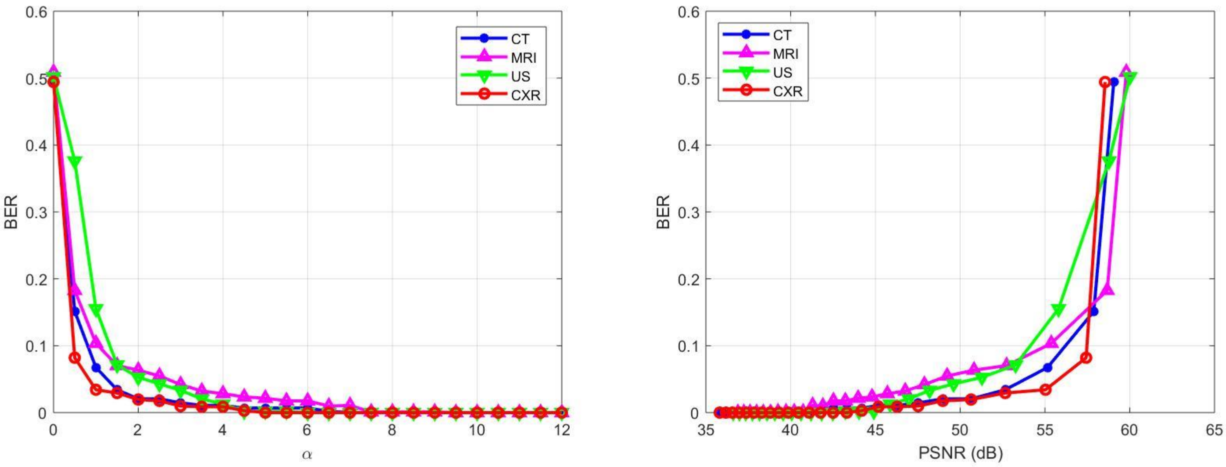

(a) (b)

Figure. 7 Evaluation of α: (a) The effect of α on BER (b) The effect of α on BER and PSNR

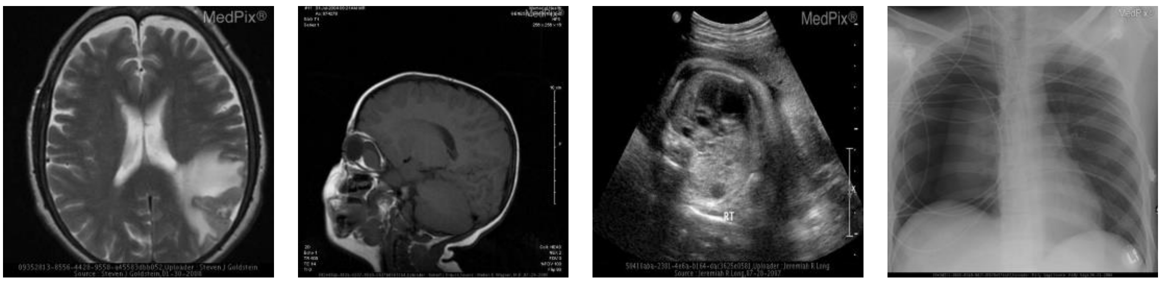

PSNR = 41.5081 dB PSNR = 40.413 dB PSNR = 43.7111 dB PSNR = 44.0064 dB

Figure. 8 Watermarked image and PSNR of each modality medical images (CT, MRI, US, X-Ray)

CT MRI US X-Ray

Recovered image

Difference between Original and Recovered image

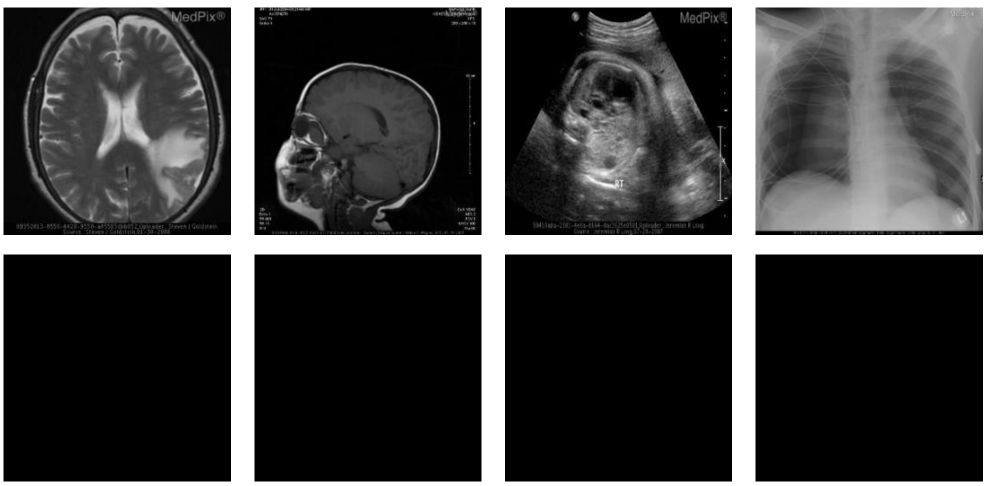

Figure. 9 Illustration of the extraction results. Rows represent recovered host medical images and also differences between original and recovered images. Columns represent the four modalities of medical imagery (CT, MRI, US, and X-ray)

Table 2. Type of attack with each parameter

Attack Type	Parameters
JPEG2000 compression (J2k)	Compression ratio=4, 8
Gaussian Noise (GN)	Mean=0.001, 0.003, 0.005, Variance=0.0001
Salt & pepper noise (SPN)	Density noise=0.001, 0.003, 0.005
Speckle Noise (SN)	Variance=0.001, 0.003, 0.005
Histogram Equalization (HE)	-
Gamma Correction (GC)	γ=0.8, 2
Sharpening (SH)	0.1, 0.2
Resize (RS)	0.8, 1.2

5.3 Robustness evaluation

This subsection evaluates how robust the proposed RRW scheme is against various attacks. Table 2 introduces the types of attacks used in the experiment: JPEG2000 compression, noise addition, image sharpening, image enhancement, and resizing. The comparison of watermark resistance performance is shown in Table 3. Meanwhile, other watermark resistance performance results are shown in Table 4.

5.3.1. JPEG2000 compression (J2k)

JPEG 2000 (J2k) is image compression and encoding system standard that offers significant codestream flexibility. J2k is one of the image processing that users widely use. Any effective watermark must be robust to a certain level of compression. The proposed RRW scheme is tested against J2k compression by modifying the compression ratio (CR) value. The CR value is inversely proportional to the file size and quality of the resulting image after compression. The higher the CR value means, the smaller the file size and the lower the image quality, so it's best. The comparison results of the recovered watermark resistance performance for J2k compression attacks with various CR are shown in Table 3. The proposed RRW scheme has superior watermark resistance under J2k compression compared to [14] and [15]. When CR=8, the watermark can still be well received by human eyes. QF=10, 20, and 30. BER=0 and NC values are close to 1, indicate that the proposed scheme is resistant to J2k compression attacks.

5.3.2. Noise addition

The most commonly discussed non-geometric attack in signal processing is noise addition. The proposed scheme evaluates watermark resistance under various types of noise, such as Gaussian (GN), salt and pepper (SPN), and speckle (SP). One of the most used statistical noise processing operations is GN. With a mean of zero, the amount of noise is varied with its variation. This RRW scheme's watermarked image has statistical noise applied to it. BER and NC values of Gaussian noise with variance = 0.001, 0.003, and 0.005 are shown in Table 3. The proposed RRW scheme is superior in watermark resistance under Gaussian noise compared to [14] and [15]. The value of BER=0 and NC=1 means that the watermark wholly recovered. The proposed scheme is resistant to Gaussian noise attacks. The main components of the proposed RRW in this paper are the independent generation of Gaussian distributed random code as a watermark mapping to the host detail subband region and applying the maximum value correlation to increase the robustness of the proposed watermarking technique.

At the time of data transmission, a pixel error causes the SPN. The noise density is calculated by changing the pixel percentage [2], and this pixel value modification gives the image a salt and pepper appearance. As shown in Table 3, this approach is evaluated against SPNs with three different noise densities. The test results show that the proposed scheme can recover the watermark image with few pixel errors. The BER value is close to 0, and the NC value is close to 1, which means that the proposed scheme is resistant to salt and pepper noise attacks.

SP is the noise that arises due to the influence of the imaging sensor during image acquisition [8]. This method is tested against SP attacks on three different noise variants. BER and NC values of SP with

Table 3. Comparison of robustness performance

Attacks	Thabit et al. [14]		Liu et al. [15]		Proposed Scheme	
	BER	**NCC**	**BER**	**NCC**	**BER**	**NCC**
J2k (4)	0.0044	0.996	0.002	0.999	**0**	**1**
J2k (8)	0.0401	0.964	0.013	0.987	**0.002**	**0.997**
GN (0.001)	0.0011	0.999	0.012	0.988	**0**	**1**
GN (0.003)	0.0012	0.998	0.072	0.988	**0**	**1**
GN (0.005)	0.0013	0.999	0.135	0.872	**0**	**1**
SPN (0.001)	0.0051	0.995	0.028	0.974	**0.002**	**0.997**
SPN (0.003)	0.0141	0.985	0.076	0.931	**0.009**	**0.989**
SPN (0.005)	0.0240	0.976	0.125	0.887	**0.009**	**0.989**
RS (0.8)	**0.0001**	**0.999**	0.006	0.997	0.059	0.921
RS (1.2)	**0**	**1**	0.001	0.999	0.020	0.969

Table 4. Evaluation of resilience under common signal processing attacks

Attacks	Proposed Scheme	
	BER	NCC
SN (0.001)	0	1
SN (0.003)	0	1
SN (0.005)	0.0020	0.9970
HE	0	1
GC (0.8)	0	1
GC (2)	0.0039	0.9940
SH (0.1)	0	1
SH (0.2)	0	1

variance = 0.001, 0.003, and 0.005 are shown in Table 4. When variance=0.001 and 0.003, BER values of 0 and NC=1, which means the watermark successfully recovered completely. When variance = 0.005, the BER and NC values are no longer ideal, but the watermark is still acceptable for authentication.

5.3.3. Geometric attack

Resizing is one of the geometric operations commonly used in the initial processing of an image. Watermarked images are manipulated by resizing attacks with resizing factors of 0.8 and 1.2 times. BER values < 20% and NC > 0.9 from watermark restoration indicate that the proposed scheme can restore watermarks with acceptable quality. Although the proposed method performs lower than [14] and [15], the results of BER and NC are still satisfactory in watermark authentication.

5.3.4. Sharpening and enhancement in image

Other types of signal processing attacks tested in this section are Histogram Equalization (HE), Gamma Correction (GC), and Image Sharpening (SH). HE is a processing technique used to increase the contrast in an image. GC can control the brightness of the entire image so that it can display the image accurately on the computer screen. Meanwhile, SH is a method that can emphasize texture and increase image focus. The performance of the modified restoration watermark under HE, GC, and SH attack with different parameter values is presented in Table 4. In the HE and SH attacks, the value of BER=0 and NC=1 means that the watermark successfully recovered completely. Whereas in GC attacks, the watermark can be restored properly when γ =0.8. The smaller the γ value means the image becomes brighter, and the texture looks more visible. Meanwhile, if the value of γ increases, the picture becomes darker, and no detail can be seen. When γ =1.2, the BER and NC values are no longer ideal, but the watermark is still acceptable for authentication.

SWT and MSS-based RRW schemes on medical images have been tested using several attacks to measure the robustness of the proposed watermarking scheme. Experimental results and performance comparisons as outlined in Table 3 and Table 4 have proven that the proposed RRW scheme is resistant to various modifications. Watermarking can be robust if the BER <20% and NC>0.9 on many attacks. Therefore, the proposed RRW scheme has acceptable imperceptibility and is said to be robust against various attacks.

The proposed RRW technique on this medical image exploits the salient properties of SWT and MSS. SWT's shift-invariance and redundancy properties are beneficial because potentially valuable image information is not removed to reproduce the image. Then, the embedding technique with MSS makes the proposed RRW can produce better imperceptibility and resistance.

6. Conclusion

This study proposes an RRW scheme with a multibit spread spectrum (MSS) embedding technique in the Stationary wavelet transform (SWT) domain. Subband diagonal detail coefficient on SWT of the host image provides better resistance than other subbands. SWT's shift-invariance and redundancy properties can restore the host image and watermark perfectly when there is no attack. The embedding technique with MSS can recover the watermark image and the host image ideally without attack. This technique provides better imperceptibility and robustness because the bits in the PN code are randomly distributed in a Gaussian distribution in each non-overlapping block. The use of the Gaussian distribution provides better watermark resistance because the Gaussian point characteristic is the part that is difficult to attack. Tests on four types of medical image modalities showed acceptable imperceptibility with a PSNR value > 41dB. Compared to other RRW schemes based on domain transform, this proposed scheme can compete and provide better resistance, especially in JPEG2000 compression attacks, noise enhancement, image sharpening, and image enhancement. Future research will develop this proposed RRW scheme by optimizing gain parameters to work adaptively, implementing medical file types from audio and video, and using encryption to ensure watermark security.

Conflicts of Interest

The authors declare no conflict of interest.

Author Contributions

Conceptualization, LDN, ABS, and GLB; methodology, LDN, ABS, DD; software, LDN and GLB; validation, ABS, and DD; formal analysis, ABS, and DD; investigation, LDN; resources, LDN; data curation, LDN; writing—original draft preparation, LDN; writing—review and editing, LDN, and ABS; visualization, LDN and GLB; supervision, ABS and DD; project administration, ABS, and DD; funding acquisition, ABS.

Acknowledgments

This research is part of L. Novamizanti's dissertation research funded by the Dissertation Doctor Research Grant from the Indonesian Ministry of Research and Technology, Indonesian Endowment Fund for Education (LPDP) Scholarships, and Telkom University. ITB also partially funded this research through the ITB research grant 2022, file number: PN-6-01-2022. L. Novamizanti is very grateful for the LPDP Scholarship, which supports his doctoral studies at ITB.

References

[1] S. Kumar and R. K. Jha, "FD-based detector for medical image watermarking", *IET Image Processing*, Vol. 13, No. 10, pp. 1773-1782, 2019.

[2] S. M. Mousavi, A. Naghsh, and S. A. R. A. Bakar, "Watermarking Techniques used in Medical Images: a Survey", *J. Digit. Imaging*, Vol. 27, No. 6, pp. 714-729, 2014.

[3] P. S. Maheshkar, "Region-based hybrid medical image watermarking for secure telemedicine applications", *Multimedia Tools and Applications*, Vol. 76, No. 3, pp. 3617-3647, 2017.

[4] K. J. Giri, Z. Jeelani, J. I. Bhat, and R. Bashir, "Survey on Reversible Watermarking Techniques for Medical Images", In: *Multimedia Security*, pp. 177-198, 2021.

[5] A. M. Ortiz, C. F. Uribe, and J. J. G. Hernandez, "A Survey on Reversible Watermarking for Multimedia Content : A Robustness Overview", *IEEE Access*, Vol. 7, pp. 132662-132681, 2019.

[6] P. Selvam, S. Balachandran, and S. Pitchai, "Hybrid transform based reversible watermarking technique for medical images in telemedicine applications", *Optik (Stuttg).*, Vol. 145, pp. 655-671, 2017.

[7] R. Thabit and B. E. Khoo, "Robust reversible watermarking scheme using Slantlet transform matrix", *J. Syst. Softw.*, Vol. 88, pp. 74-86, 2014.

[8] C. Yang, P. Liu, G. Yin, H. Jiang, and X. Li, "Defect detection in magnetic tile images based on stationary wavelet transform", *NDT&E Int.*, Vol. 83, pp. 78-87, 2016.

[9] G. Budiman, A. B. Suksmono, D. Danudirdjo, and S. Pawellang, "QIM-based Audio Watermarking with Combined Techniques of SWT-DST-QR-CPT Using SS-based Synchronization", In: *Proc. of 2018 6th International Conference on Information and Communication Technology*, pp. 286-292, 2018.

[10] A. Setyono and D. R. I. M. Setiadi, "An Image Watermarking Method Using Discrete Tchebichef Transform and Singular Value Decomposition Based on Chaos Embedding", *International Journal of Intelligent Engineering and Systems*, Vol. 13, No. 2, pp. 140-150, 2020, doi: 10.22266/ijies2020.0430.14.

[11] L. Novamizanti, I. Wahidah, and N. P. D. P. Wardana, "A Robust Medical Images Watermarking Using FDCuT-DCT-SVD", *International Journal of Intelligent Engineering and Systems*, Vol. 13, No. 6, pp. 266-278, 2020, doi: 10.22266/ijies2020.1231.24.

[12] A. A. Mohammed, M. A. M. Abdullah, S. R. Awad, and F. S. Alghareb, "A Novel FDCT-SVD Based Watermarking with Radon Transform for Telemedicine Applications", *International Journal of Intelligent Engineering and Systems*, Vol. 15, No. 1, 2022, doi: 10.22266/ijies2022.0228.07.

[13] R. Thabit and B. E. Khoo, "Medical image authentication using SLT and IWT schemes", *Multimedia Tools and Applications*, Vol. 76, No. 1, pp. 309-332, 2017.

[14] R. Bamal and S. S. Kasana, "Slantlet based hybrid watermarking technique for medical images", *Multimedia Tools and Applications*, Vol. 77, No. 10, pp. 12493-12518, 2018.

[15] X. Liu, "Scheme for Protecting Authenticity and Integrity of Medical Images", *IEEE Access*, Vol. 7, pp. 76580-76598, 2019.

[16] X. Wang, X. Li, and Q. Pei, "Independent Embedding Domain Based Two-Stage Robust Reversible Watermarking", *IEEE Trans. Circuits Syst. Video Technol.*, Vol. 30, No. 8, pp. 2406-2417, 2020.

[17] P. V. Nagarjuna, "Robust Blind Digital Image Watermarking Scheme Based on Stationary Wavelet Transform", *2013 Sixth Int. Conf. Contemp. Comput.*, pp. 451-454, 2013.

[18] Q. Dai, J. Li, U. A. Bhatti, Y. W. Chen, and J.

Liu, “SWT-DCT-based robust watermarking for medical image”, *Innovation in Medicine and Healthcare Systems, and Multimedia*, pp. 93-103, 2019.

[19] B. Kumar, S. B. Kumar, and D. S. Chauhan, “Wavelet Based Imperceptible Medical Image Watermarking Using Spread-Spectrum”, In: *Proc. of 2015 38th International Conference on Telecommunications and Signal Processing (TSP)*, pp. 1-5, 2015.

[20] S. P. Maity and M. K. Kundu, “Performance Improvement in Spread Spectrum Image Watermarking using Wavelets”, *International Journal of Wavelets, Multiresolution and Information Processing*, Vol. 9, No. 1, pp. 1-33, 2011.

[21] A. Samčović and M. Milovanović, “Robust Digital Image Watermarking Based on Wavelet Transform and Spread Spectrum Techniques”, *2015 23rd Telecommunications Forum Telfor*, pp. 811-814, 2015.

[22] R. Thanki, A. Kothari, and D. Trivedi, “Hybrid and blind watermarking scheme in DCuT – RDWT domain”, *J. Inf. Secur. Appl.*, Vol. 46, pp. 231-249, 2019.

[23] Y. O. Xin and M. I. Pawlak, “M -Ary Phase Modulation for Digital Watermarking”, *International Journal of Applied Mathematics and Computer Science*, Vol. 18, No. 1, pp. 93-104, 2008.

[24] Y. Xiang, I. Natgunanathan, D. Peng, G. Hua, and B. Liu, “Spread Spectrum Audio Watermarking Using Multiple Orthogonal PN Sequences and Variable Embedding Strengths and Polarities”, *IEEE/ACM Transactions on Audio, Speech, and Language Processing*, Vol. 26, No. 3, pp. 529-539, 2018.

[25] G. Budiman, A. B. Suksmono, and D. Danudirdjo, “Compressive Sampling with Multiple Bit Spread Spectrum-Based Data Hiding”, *Appl. Sci.*, Vol. 10, No. 12, pp. 1-21, 2020.

[26] National Library of Medicine, “Medical Image Database.”, https://medpix.nlm.nih.gov/home (accessed Nov. 01, 2021).

[27] R. Bamal and S. S. Kasana, “Slantlet based hybrid watermarking technique for medical images”, *Multimedia Tools and Applications*, Vol. 77, No. 10, pp. 12493-12518, 2018.